Supporting Information

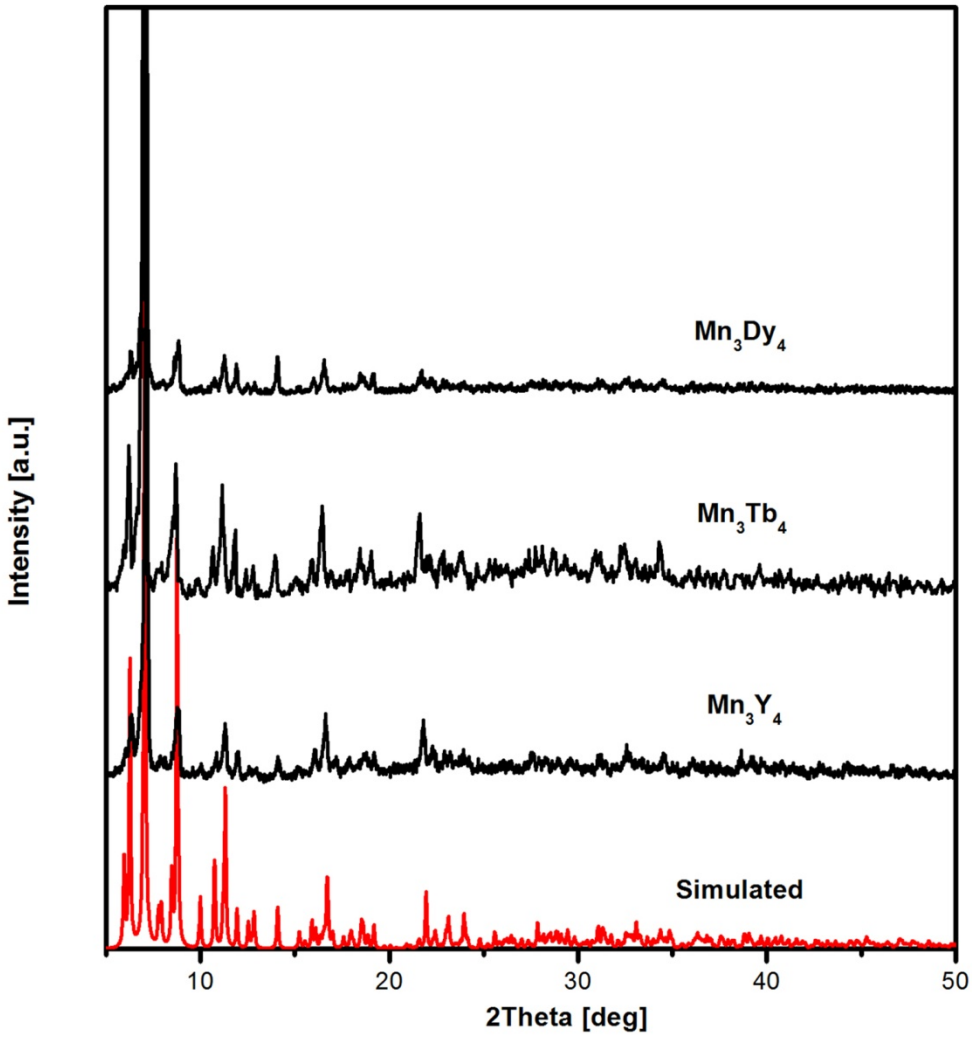

Figure S1. The simulated XRPD pattern and the experimental patterns for complexes **1**-**3**.

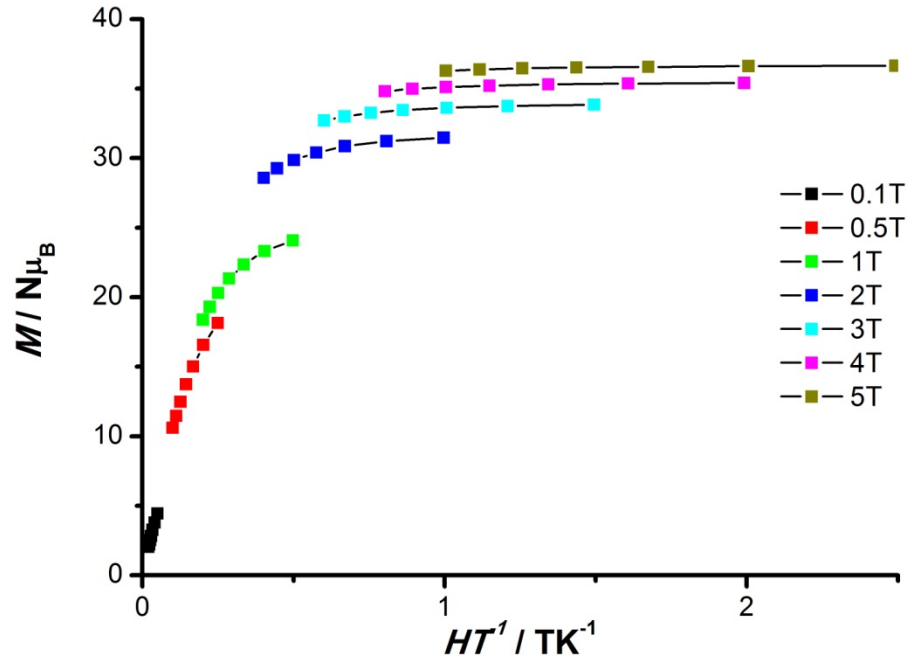

Figure S2. Plots of $M/N\mu_B$ vs H/T for complex **1** (Mn_3Dy_4) at the indicated applied fields. Solid lines are eye guides.

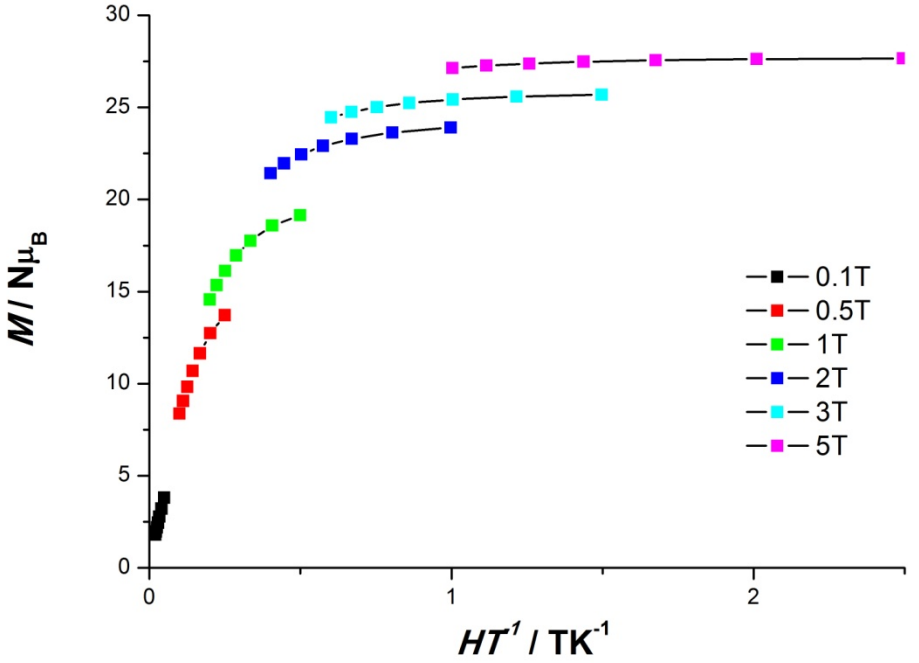

Figure S3. Plots of $M/N\mu_B$ vs H/T for complex **2** (Mn_3Tb_4) at the indicated applied fields. Solid lines are eye guides.

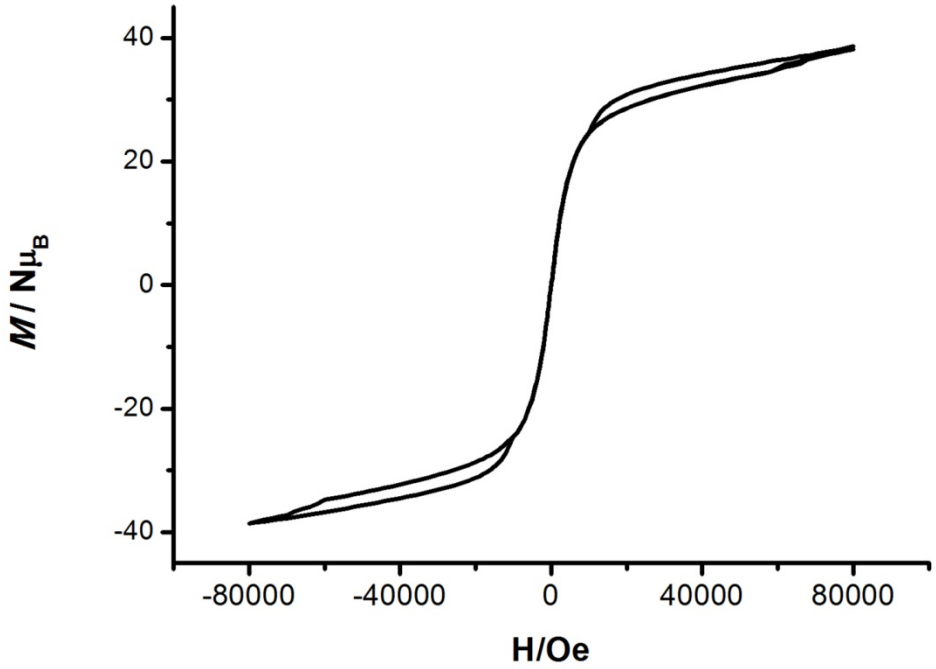

Figure S4. Plots of $M/N\mu_B$ vs H for complex **1** at 2K.

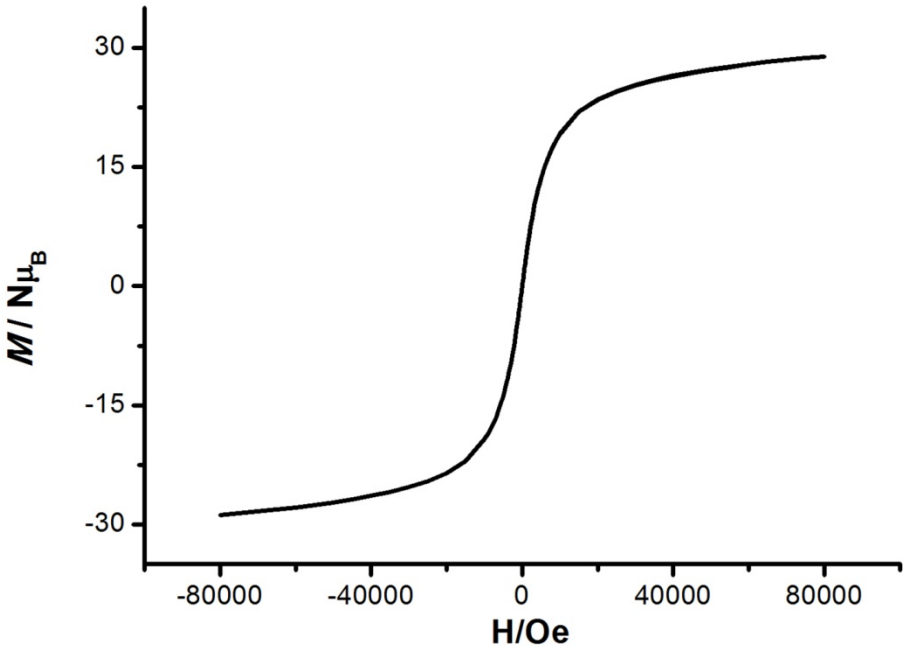

Figure S5. Plots of $M/N\mu_B$ vs H for complex **2** at 2K.

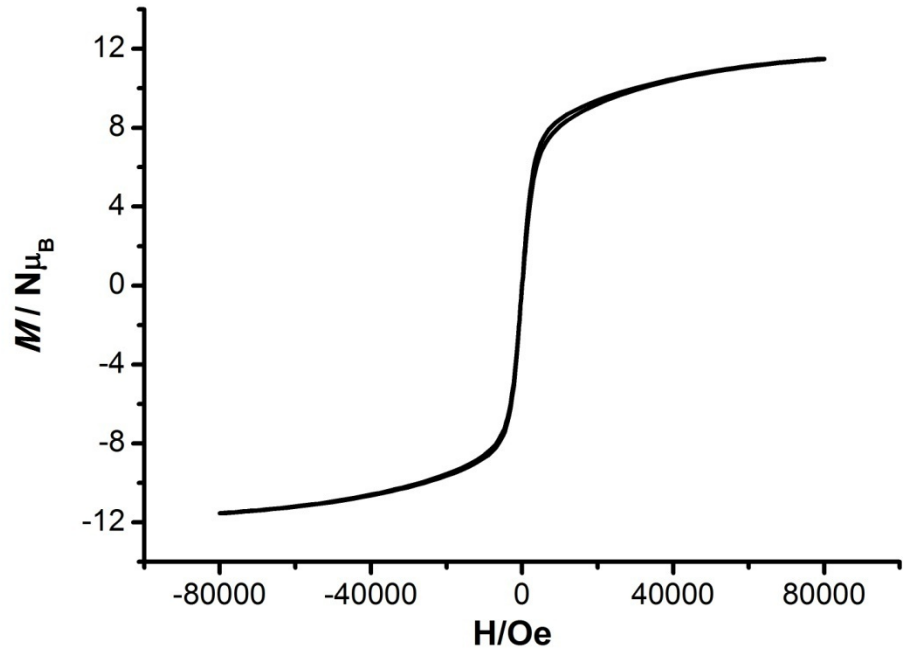

Figure S6. Plots of $M/N\mu_B$ vs H for complex **3** at 2K.

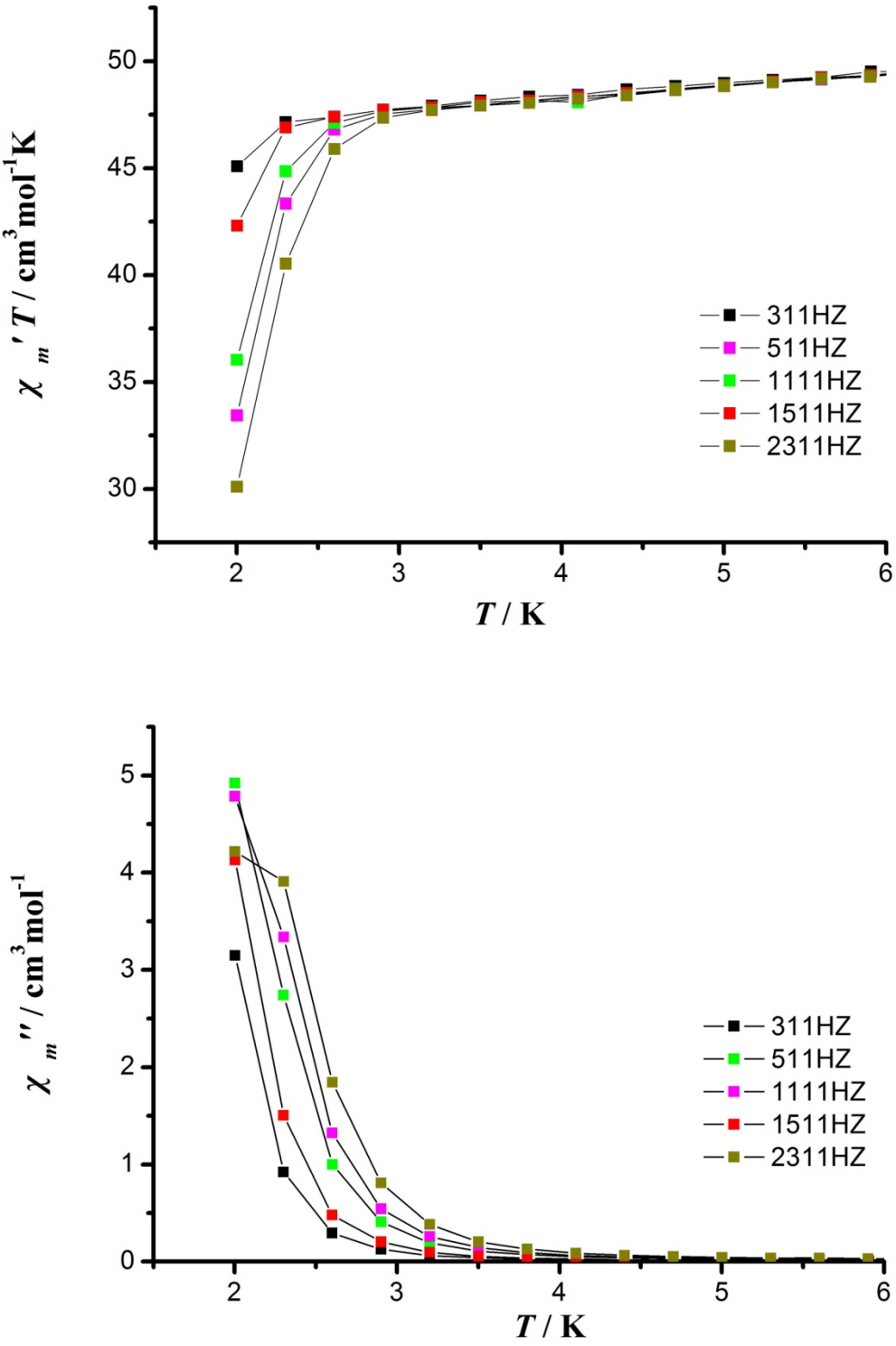

Figure S7. In-phase (shown as $\chi'_{m}T$) and out-of-phase (χ''_{m}) ac susceptibility signals of complex **2** oscillating at the indicated frequencies at H_{ac} = 3.0G and H_{dc} = 0.

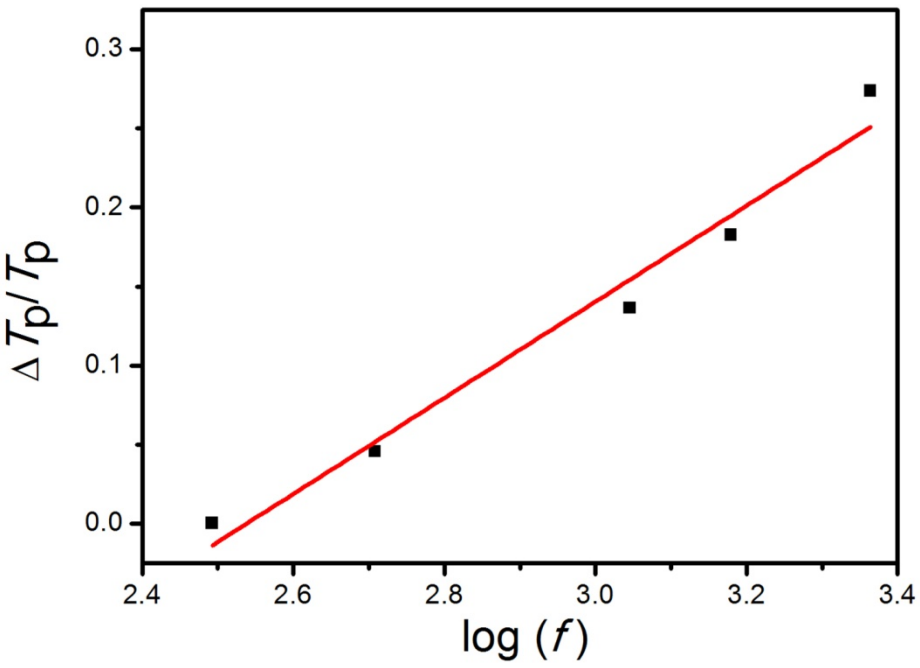

Figure S8. The log(f) vs. ΔTp/Tp plots for complex **1**. The value of φ can be extracted from the slope.

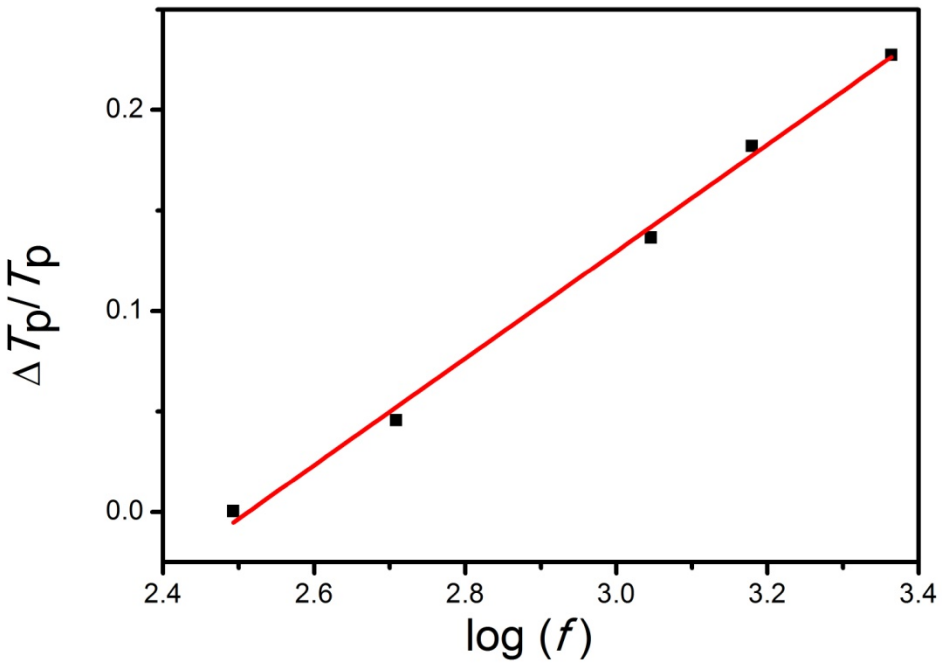

Figure S9. The log(*f*) vs. Δ*T*p/*T*p plots for complex **3**. The value of φ can be extracted from the slope.